

Shape-memory polymers as flexible resonator substrates for continuously tunable organic DFB lasers

Senta Schauer,¹ Xin Liu,² Matthias Worgull,¹ Uli Lemmer,^{1,2} and Hendrik Hölscher,^{1,*}

¹*Institute of Microstructure Technology (IMT), Karlsruhe Institute of Technology (KIT), Hermann-von-Helmholtz-Platz 1, 76344 Eggenstein-Leopoldshafen, Germany*

²*Light Technology Institute (LTI), Karlsruhe Institute of Technology (KIT), Engesserstrasse 13, 76131 Karlsruhe, Germany*

**Hendrik.Hoelscher@kit.edu*

Abstract: We introduce shape-memory polymers (SMP) as substrate material for active optical devices. As an exemplary application we build a tunable organic semiconductor distributed feedback (DFB) laser. Hence, we transfer a second order Bragg grating with a period of 400 nm into SMP foils by hot embossing. The composite organic gain medium Alq₃:DCM evaporated on the SMP substrate serves as laser active material. Mechanical stretching of the substrate increases the grating period temporarily and triggering the shape-memory effect afterwards reduces the period on demand. In this way, we can adjust the grating period to achieve a broad continuously tuning of the laser emission wavelength by 30 nm.

© 2015 Optical Society of America

OCIS codes: (140.3490) Lasers, distributed-feedback; (140.3410) Laser resonators; (160.5470) Polymers; (160.6840) Thermo-optical materials.

References and links

1. A. Lendlein and R. Langer, "Biodegradable, elastic shape-memory polymers for potential biomedical applications," *Science* **296**, 1673–1676 (2002).
2. A. Lendlein and S. Kelch, "Shape memory polymers," *Angew. Chemie* **41**, 034 – 2057 (2002).
3. D. Ratna and J. Karger-Kocsis, "Recent advances in shape memory polymers and composites: a review," *J. Mater. Sci.* **43**, 254–269 (2008).
4. Q. Meng and J. Hu, "A review of shape memory polymer composites and blends," *Composites* **40**, 1661–1672 (2009).
5. A. Lendlein, *Shape-Memory Polymers* (Springer, Berlin, 2010).
6. T. Xie, "Recent advances in polymer shape memory," *Polymer* **52**, 4985–5000 (2011).
7. J. Leng, X. Lan, Y. Liu, and S. Du, "Shape-memory polymers and their composites: Stimulus methods and applications," *Prog. Mater. Sci.* **56**, 1077–1135 (2011).
8. C. M. Yakacki, R. Shandas, C. Lanning, B. Rech, A. Eckstein, and K. Gall, "Unconstrained recovery characterization of shape-memory polymer networks for cardiovascular applications," *Biomaterials* **28**, 2255–2263 (2007).
9. H. Xu, C. Yu, S. Wang, V. Malyarchuk, T. Xie, and J. A. Rogers, "Deformable, programmable, and shape-memorizing micro-optics," *Adv. Funct. Mater.* **23**, 3299–3306 (2013).
10. A. Espinha, M. C. Serrano, and A. Blanco, "Thermoresponsive shape-memory photonic nanostructures," *Adv. Optical Mat.* **2**, 516–521 (2014).
11. N. Schneider, C. Zeiger, A. Kolew, M. Schneider, J. Leuthold, H. Hölscher, and M. Worgull, "Nanothermoforming of hierarchical optical components utilizing shape memory polymers as active molds," *Opt. Mater. Express* **4**, 1895 (2014).
12. D. Schneider, T. Rabe, T. Riedl, T. Dobbertin, M. Kröger, E. Becker, H.-H. Johannes, W. Kowalsky, T. Weimann, J. Wang, P. Hinze, A. Gerhard, P. Stössel, and H. Vestweber, "An ultraviolet organic thin-film solid-state laser for biomarker applications," *Adv. Mater.* **17**, 3134 (2005).

13. Y. Oki, S. Miyamoto, M. Maeda, and N. Vasa, "Multiwavelength distributed-feedback dye laser array and its application to spectroscopy," *Opt. Lett.* **27**, 1220–1222 (2002).
14. T. Woggon, S. Klinkhammer, and U. Lemmer, "Compact spectroscopy system based on tunable organic semiconductor lasers," *Appl. Phys. B* **99**, 47–51 (2010).
15. S. Klinkhammer, T. Woggon, C. Vannahme, U. Geyer, T. Mappes, and U. Lemmer, "Optical spectroscopy with organic semiconductor lasers," *Appl. Phys. B* **99**, 47–51 (2010).
16. X. Liu, P. Stefanou, B. Wang, T. Woggon, T. Mappes, and U. Lemmer, "Organic semiconductor distributed feedback (dfb) laser as excitation source in raman spectroscopy," *Opt. Express* **21**, 28941–28947 (2013).
17. X. Liu, S. Lebedkin, T. Mappes, S. Köber, C. Koos, M. Kappes, and U. Lemmer, "Organic semiconductor distributed feedback laser as excitation source in raman spectroscopy using free-beam and fibre coupling," *Opt. Express* **21**, 28941–28947 (2013).
18. T. Voss, D. Scheel, and W. Schade, "A microchip-laser-pumped dfb-polymer-dye laser," *Appl. Physics B* **73**, 105–109 (2001).
19. K. Suzuki, K. Takahashi, Y. Seida, K. Kumagai, and Y. Taniguchi, "A continuously tunable organic-solid state laser based on a flexible distributed-feedback resonator," *Jpn. J. Appl. Phys.* **42**, L249–L251 (2003).
20. M. R. Weinberger, G. Langer, A. Pogantsch, A. Haase, E. Zojer, and W. Kern, "Continuously color tunable rubber laser," *Adv. Mater.* **16**, 130–133 (2004).
21. B. Wenger, N. Tétreault, M. E. Welland, and R. H. Friend, "Mechanically tunable conjugated polymer distributed feedback lasers," *Appl. Phys. Lett.* **19**, 193303 (2010).
22. P. Görrn, M. Lehnhardt, T. R. W. Kowalsky and, and S. Wagner, "Elastically tunable self-organized organic lasers," *Adv. Mater.* **23**, 869–872 (2011).
23. S. Döring, M. Kollösche, T. Rabe, J. Stumpe, and G. Kofod, "Electrically tunable polymer DFB laser," *Adv. Mater.* **23**, 4265–4269 (2011).
24. J. Wang, T. Weimann, P. Hinze, G. Ade, D. Schneider, T. Rabe, T. Riedel, and W. Kowalsky, "A continuously tunable organic dfb laser," *Microelectron. Eng.* **78–79**, 364–368 (2005).
25. Z. Li, Z. Zhang, A. Scherer, and D. Psaltis, "Mechanically tunable optofluidic distributed feedback dye laser," *Opt. Express* **14**, 10494–10499 (2006).
26. F. B. Arango, M. B. Christiansen, M. Gersborg-Hansen, and A. Kristensen, "Optofluidic tuning of photonic crystal band edge lasers," *Appl. Phys. Lett.* **91**, 223503 (2007).
27. S. Klinkhammer, T. Woggon, U. Greyer, C. Vannahme, T. Mappes, S. Dehm, and U. Lemmer, "A continuously tunable low-threshold organic semiconductor distributed feedback laser fabricated by rotating shadow mask evaporation," *Appl. Phys. B* **97**, 787–791 (2009).
28. S. Klinkhammer, X. Liu, K. Huska, Y. Shen, S. Vanderheiden, S. Valouch, C. Vannahme, S. Bräse, T. Mappes, and U. Lemmer, "Continuously tunable solution-processed organic semiconductor dfb lasers pumped by laser diode," *Opt. Express* **20**, 6357–6364 (2012).
29. R. Ozaki, T. Shinpo, K. Yoshino, M. Ozaki, and H. Moritake, "Tunable liquid crystal laser using distributed feedback cavity fabricated by nanoimprint lithography," *Appl. Phys. Express* **1**, 012003 (2008).
30. S. Klinkhammer, N. Heussner, K. Huska, T. Bocksrocker, F. Geiselhöringer, C. Vannahme, T. Mappes, and U. Lemmer, "Voltage controlled tuning of an organic semiconductor distributed feedback laser using liquid crystals," *Appl. Phys. Lett.* **99**, 023307 (2011).
31. I. D. W. Samuel and G. A. Turnbull, "Organic semiconductor lasers," *Chemical Reviews* **107.4**, 1272–1295 (2007).
32. M. Worgull, *Hot Embossing - Theory and Technology of Microreplication* (Micro and Nano Technologies, Elsevier Science, William Andrew, Norwich, NY, 2009).
33. V. Saile, U. Wallrabe, O. Tabata, and J. G. Korvink, eds., *LIGA and Its Applications* (Wiley-VCH, Weinheim, 2009).
34. S. Klinkhammer, "Durchstimmbare organische Halbleiter," Ph.D. thesis, Karlsruhe Institute of Technology, Karlsruhe, Germany (2011).
35. C. Vannahme, S. Klinkhammer, A. Kolew, P.-J. Jakobs, M. Guttman, S. Dehm, U. Lemmer, and T. Mappes, "Integration of organic semiconductor lasers and single-mode passive waveguides into a pmma substrate," *Microelectron. Eng.* **87**, 693–695 (2010).
36. C. Vannahme, S. Klinkhammer, U. Lemmer, and T. Mappes, "Plastic lab-on-a-chip for fluorescence excitation with integrated organic semiconductor lasers," *Opt. Express* **19**, 8179–8186 (2011).

1. Introduction

Smart polymers and applications thereof received rising attention during the last decade. [1–7]. These polymers respond autonomously to external stimuli by changing their state, properties or shape. Polymers changing their macroscopic shape in a predefined way when triggered by a proper stimulus are shape-memory polymers (SMPs) [2]. Those polymers were already exten-

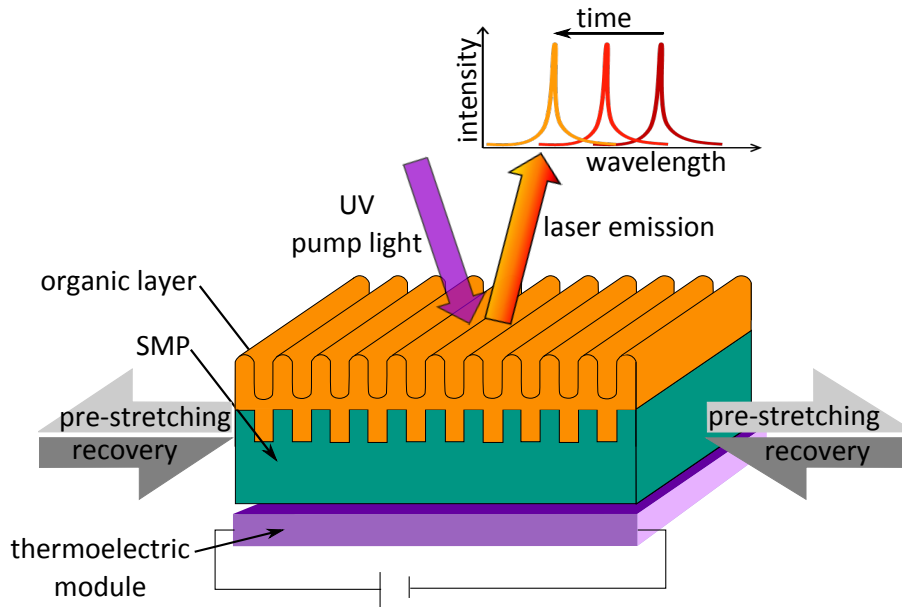


Fig. 1. Schematic of a tunable organic semiconductor distributed feedback laser device consisting of a nanostructured flexible substrate made of shape-memory polymers and an organic laser active layer. The shape-memory polymer substrate features a hot embossed second order Bragg surface grating as resonator and is mechanically pre-stretched. The organic semiconductor material Alq₃:DCM serves as laser active medium. While the device is heated by the thermoelectric module, the smaller original grating period recovers and the grating period as well as the emission wavelength of the device are adjustable.

sively studied for macroscopic applications, e.g., for deployable components in aerospace [7], medical applications like self-unfolding stents, [8] or shape-memory sutures [1]. However, there are several applications where micro- or nano-structured active polymer devices are advantageous [9–11], e.g., as tunable nanostructured resonator substrates for optical devices.

Since the demonstration of a UV tunable organic distributed Bragg reflector (DBR) laser as excitation source for biomarker experiments by Schneider *et al.* [12], organic solid-state lasers have attracted attention as potential light sources for spectroscopic applications. Organic solid-state lasers offer widely tunable laser radiation over the UV and the visible range and this unique advantage might solve spectroscopy issues. Up to now, organic semiconductor lasers have been successfully applied in fluorescence excitation, [12] absorption spectroscopy [13], transmission spectroscopy [14, 15], and Raman spectroscopy [16, 17]. Temperature tuning [18], mechanical stretching of rubber-like grating substrates [19–23], chirped gratings [24], optofluidics [25, 26], wedged shaped films [27, 28], or special properties of liquid crystals [29, 30] have been investigated to tune the emission wavelength of organic distributed feedback (DFB) lasers, recently. However, for the fabrication of rigid chirped gratings, time-consuming lithography is needed for every substrate [24, 26] while state-of-the-art rubber-like grating substrates depend on complex rigid set-ups for adjustment [18, 26] or elaborate mechanical supports [19–22, 24, 25, 27, 28]. These constraints are avoided with gratings made out of SMPs.

Here, we demonstrate an organic DFB laser featuring a mechanically pre-stretched SMP substrate with a surface Bragg grating as resonator structure. The thermal evaporation of a thin organic active layer onto this substrate and a thermoelectric module accomplish the whole laser

device. Figure 1 shows the schematic set-up of our device. According to the Bragg equation each resonator period Λ amplifies a specific laser wavelength λ_{Bragg} [31]

$$\lambda_{\text{Bragg}} = \frac{2}{m} n_{\text{eff}} \Lambda, \quad (1)$$

where n_{eff} and m are the effective refractive index and the Bragg grating order, respectively. Thus, the emission wavelength λ_{Bragg} is proportional to the resonator period Λ and we modify the resonator's period by thermally activating the shape-memory effect to tune the laser wavelength. In this way, we continuously reduce the grating period from 440 nm to 400 nm whereby the emission wavelength of the laser shift from 630 nm to 600 nm, resulting in an overall shift of 30 nm. In the following, we describe the basic features of the SMP grating structure and analyze the properties of a continuously tunable DFB laser build with this component.

2. Experimental

The ability of SMP to perform a macroscopic shape change is caused by their molecular structure [2,5]. The shape-memory effect is present in various block copolymers if the different chain blocks arrange segregated and form thereby two types of segments. Depending on the strength of intermolecular interaction forces within those segments they exhibit diverse glass transition temperatures. The segments with the higher glass transition temperature T_{hard} are termed hard segments also called netpoints whereas the segments with the lower glass transition temperature T_{switch} are termed softer switching segments. To enable the shape-memory effect, the polymer has to go through a programming cycle [1, 5]. In the original, permanent shape the netpoints are linked with each other by switching segments in their unstressed, lowest energy conformation (Fig. 2a). Assuming a thermoplastic polymer, one can define a new permanent shape of the sample by deforming it above T_{hard} where the netpoints are released. The programming of the temporary shape has to take place below T_{hard} to leave the netpoints unaffected and only the switching segments are released. Therefore, elongation of a piece of SMP at $T < T_{\text{hard}}$ leads to extended, tensioned switching segments, whose polymer chains are uncoiled and transferred into a higher energy conformation state (Fig. 2b). Cooling the polymer in this shape increases the intermolecular interaction forces. This procedure stabilizes the temporary shape to such an extent that releasing the external strain leads to almost no shape change. As soon as the temporarily shaped polymer is heated above the switching temperature T_{switch} the mobility of the polymer chains increases and the stored mechanical energy is released. Back in the lowest energy conformation, all the polymer chains feature the same lengths as in the initial permanent shape. Thus, the netpoints are in their primary positions leading to the original macroscopic shape again (Fig. 2a).

The SMP we utilized for our experiments is Tecoflex[®] EG-72D from Lubrizol (Ohio, USA). It is a completely amorphous thermoplastic polyurethane block-copolymer. As a thermoplastic polymer it is suitable for common polymer processing techniques and due to its amorphous structure Tecoflex[®] is transparent in the visible regime (about 90% for all wavelengths between 370 nm to 800 nm). In Tecoflex[®] the hard segments consist of blocks of 1-isocyanato-4-[(4-isocyanatocyclohexyl)methyl]cyclohexane (H₁₂MDI) together with 1,4-butanediol (1,4-BD). H₁₂MDI plus poly(tetramethylene ether) glycol (PTMEG) blocks build the softer switching segments. The upper and lower glass transition temperatures were experimentally identified by differential scanning calorimetry (DSC) and dynamic-mechanical analysis (DMA) as $T_{\text{hard}} \approx 150^\circ\text{C}$ and $T_{\text{switch}} \approx 40 - 60^\circ\text{C}$.

To fabricate SMP resonator substrates out of the Tecoflex[®] granulate material we used hot embossing to replicate 2nd order one-dimensional Bragg gratings. The hot embossing technique [32] allows to control precisely applied temperatures, position of tool and substrate plate,

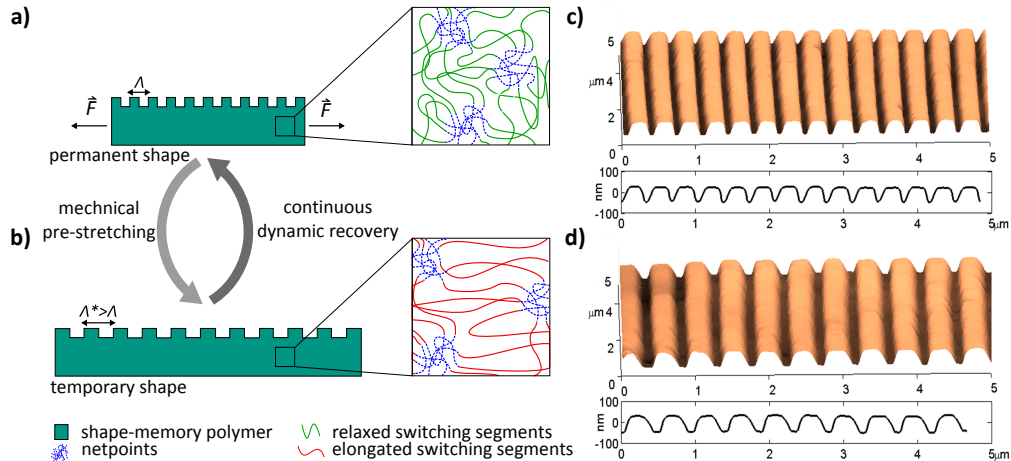


Fig. 2. **a)** The permanent shape of the SMP resonator with the grating period Λ possess netpoints linked with each other by completely relaxed switching segments. **b)** By mechanically stretching the SMP foils the period increases to Λ^* and on the molecular level the switching segments get elongated and fixed in a new shape. **c)** The fabrication of such a surface grating by hot embossing leads to uniformly replicated grating with a period of 400 nm. **d)** After stretching the grating, the enlarged period of 440 nm is evenly distributed over the whole substrate as revealed by the AFM topography image.

embossing pressure and velocity during structuring the polymer foils. Limited basically by size and quality of the mold insert, we can replicate 2.5-dimensional structures of centimeter to nanometer dimensions into various polymers. For hot embossing Tecoflex[®] we used a nickel mold insert with various linear gratings, which was fabricated with the LIGA-process [33]. To define the grating with a period of $\Lambda = 400$ nm as the permanent shape, the hot embossing temperature for Tecoflex[®] was chosen slightly above T_{hard} as 155°C. The surface of the resulting sample was imaged by atomic force microscopy (AFM) (see Fig. 2c)). Programming the temporary shape was achieved by stretching the SMP substrates perpendicularly to the grating orientation in a tensile testing machine (INSTRON 4505). In this way, we increased the grating period to $\Lambda^* \approx 440$ nm (Fig. 2d)). Afterwards a thin layer of organic laser active material was evaporated on top of those stretched samples in a high vacuum coating plant (Lesker Spectros, Kurt J. Lesker Company) [34]. We deployed the host-guest small molecule blend Aluminium-tris(8-hydroxyquinolin)(Alq₃) doped with 2-3 % 4-(dicyanomethylene)-2-methyl-6-(p-dimethylaminostyryl)-4H-pyran (DCM) [34] as our laser active medium. The evaporated layer thickness was about 235 nm.

For optical characterization we used a diode-pumped, actively Q-switched frequency-tripled neodymium-doped yttrium orthovanadate (Nd:YVO₄) laser (Advanced Optical Technology Ltd., AOT.YVO.20QSP) with a wavelength of 355 nm and a pulse duration of 0.5 ns to excite the samples. The pump pulse energy was adjusted with a variable neutral density filter and measured with a calibrated gallium arsenide phosphide (GaAsP) photodiode connected to an oscilloscope. The sample was kept in a vacuum chamber ($\approx 10^{-3}$ Pa) to protect the active material from photooxidation. The chamber can be moved perpendicular to the pump beam using an automated precision stage. This feature allows a spectrally and spatially resolved characterization of the sample. The laser beam emitted by the device is guided by several optics to a multimode fiber leading to a spectrograph (Acton Research Corporation, SpectraPro 300i)

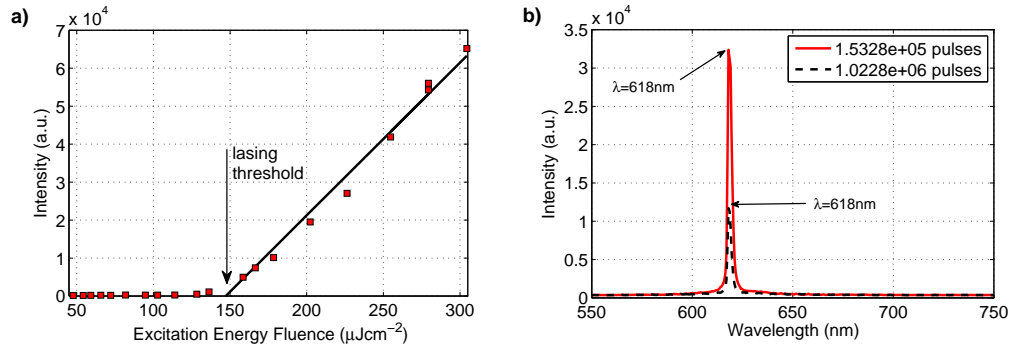


Fig. 3. **a)** Input-output characteristics used to determine the lasing threshold which was observed at $\approx 150 \mu\text{Jcm}^{-2}$. **b)** The laser spectra measured after $1.5 \cdot 10^5$ and 10^6 pump pulses under non-stop optical pumping. The pump energy does not trigger the recovery process though degradation of the organic material led to a decreased lasing intensity.

connected to an intensified charge-coupled device (ICCD) camera (Princeton Instruments, Pi-Max 512). To trigger the shape-memory effect later on, we mounted a thermoelectric module beneath the sample holder and a temperature sensor was fixed at the module to perceive the instantaneous temperature.

3. Results and discussion

To determine the optimal resonator period for the combination of Tecoflex[®] and Alq₃:DCM we analyzed devices with grating periods between 180 nm to 460 nm (10 nm steps). After evaporation of the organic Alq₃:DCM layer we examined the lasing intensity in this range and observed lasing for periods between 390 nm to 450 nm (data not shown). In order to operate our final device within this window of suitable grating periods, we choose a period of 400 nm for the permanent shape of the gratings and pre-stretched them to 440 nm for the following experiments. Since we tune the DFB laser by modifying the resonator's period, the evaporated organic Alq₃:DCM layer may be mechanically deformed by the pre-stretching of the substrate for the programming of the temporary shape as well as during the recovery process. To analyze any unwanted wear of the active layer by this mechanical strain we evaporated a 235 nm thick Alq₃:DCM layer on top of SMP gratings before and after mechanical stretching. Stretching after evaporation led to several cracks in the Alq₃:DCM layer while vice versa processed samples exhibited almost no change of the active layer after compression due to the recovery process (data not shown). Consequently, we used the second option to build the organic DFB laser devices presented in the following.

The lasing threshold of our device was observed at $150 \mu\text{J cm}^{-2}$ (Figure 3a). This value is comparable to Alq₃:DCM laser devices built on polymer substrates from poly(methyl methacrylate) (PMMA) and cyclic-olefin-copolymer (COC) [35, 36]. In order to prove that the energy of the pump laser does not initialize the recovery process of Tecoflex[®] we measured the performance of a stretched device (Fig. 3b)). Under non-stop optical pumping with an excitation energy of 150 nJ per pulse and a repetition rate of 5 kHz, we observed that the laser intensity decreased slightly after 10^6 pulses due to photo-degradation. However, the laser emission wavelength stayed at 618 nm. This outcome demonstrates that the shape-memory effect is not triggered by the UV-excitation and hence the grating period stays constant.

Figure 4 shows the tuning of the emission wavelength by changing the period of the shape-memory resonator. Here, we initialized the dynamic and continuous recovery of the original

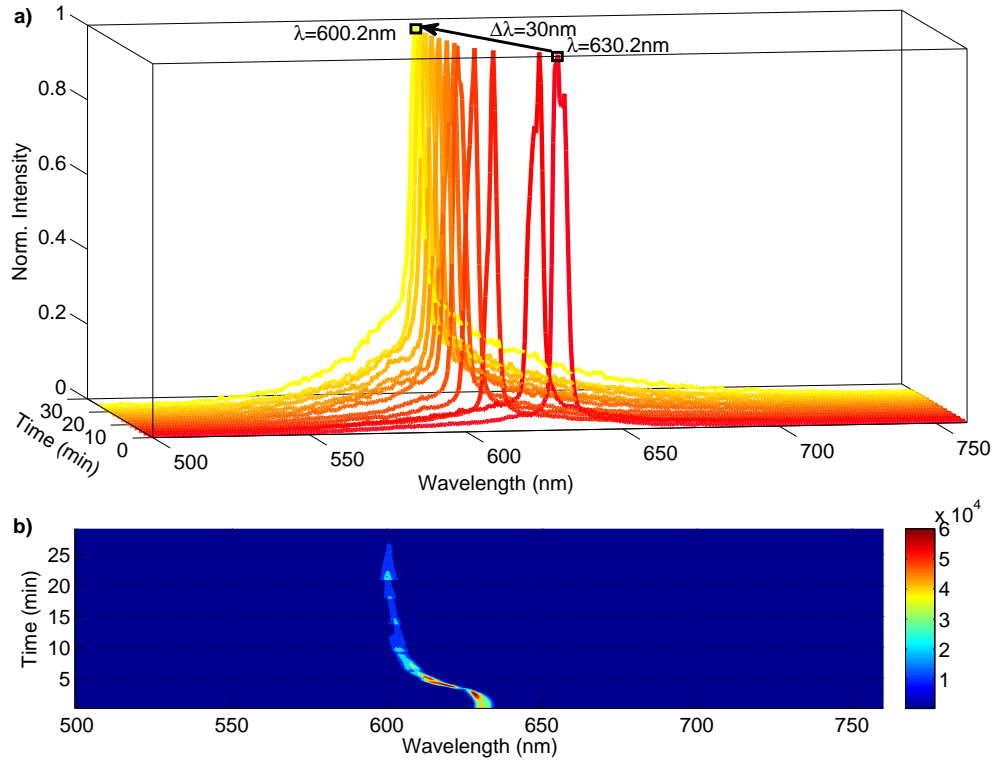


Fig. 4. **a)** The wavelength shift from 630.2 nm to 600.2 nm is shown by several emission spectra recorded during the recovery process of a heated SMP grating substrate with Alq₃:DCM. The grating period was pre-stretched by 10 % to 440 nm. **b)** The false color image of the same data demonstrates the shift and the decreasing intensity of the emission peak with time.

grating period by heating the SMP grating substrate above T_{switch} to 69° C. As mentioned before the grating was pre-stretched to a period of 440 nm. During this process we recorded the emission spectra, as shown in Fig. 4a). The stretched grating period corresponds to the right-most spectrum with the peak emission wavelength of $\lambda = 630.2$ nm. In order to illustrate the temperature dependent recovery rate, we plotted spectra separated by equal time intervals of $\Delta t = 2$ min. The emission wavelength did not change until the temperature approached T_{switch} . Henceforward, the shape recovery accelerated with rising temperature until the thermoelectric module reached the maximum temperature of 69° C. The recovery process ceased with approaching the original grating period of 400 nm and the shift of the emission wavelength ended in the leftmost spectra with an emission peak at $\lambda = 600.2$ nm. Thus, we achieved an overall wavelength shift of $\Delta\lambda = 30$ nm with this device. Figure 4b) depicts the complete wavelength shift of this experiment in a false color image. The color code in this diagram allows the observation of the diminishing lasing intensity which is caused by two reasons: the organic gain medium Alq₃:DCM degraded and the laser wavelength approached to a lower gain spectral range of Alq₃:DCM.

Shape-memory polymers as resonator material enable not only the continuous decrease of the grating period. They also allow to adjust the laser emission to a constant wavelength arbitrarily chosen from the suitable spectral range (600 nm to 630 nm in our case). To demonstrate

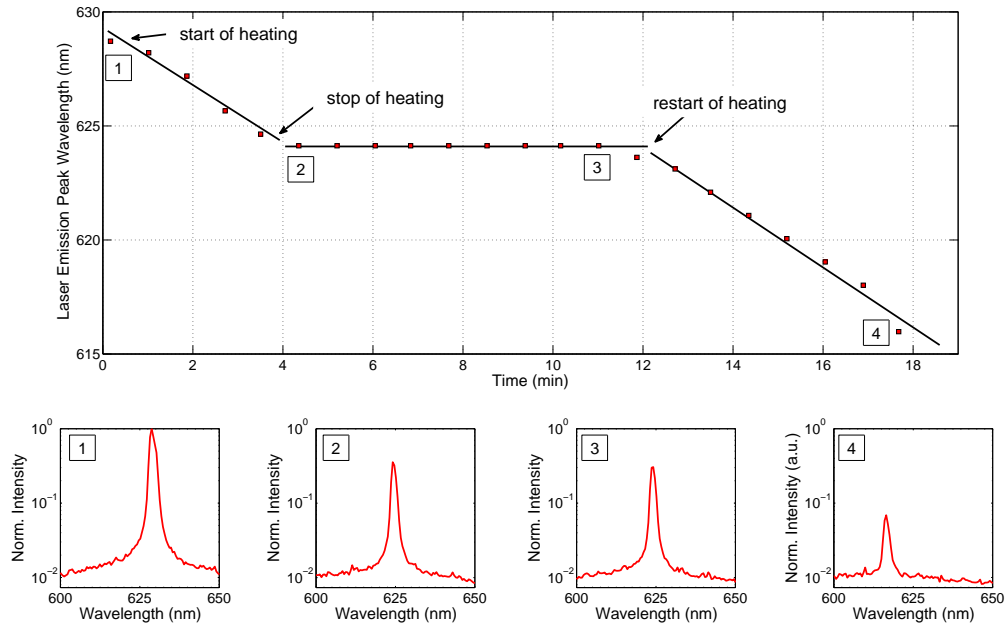


Fig. 5. The temperature dependence of the shape recovery process can be used to adjust the emission wavelength to a previously chosen value. After heating the sample the emission wavelength decreased until we switched off the thermoelectric module, by what the temperature decreased and the recovery process stopped. As a result the emission wavelength stayed constant as long as the device was exposed to temperatures lower than T_{switch} . After switching on the thermoelectric module, the temperature raised again, the recovery process continued and the emission wavelength decreased with approximately the same velocity as before. The laser spectra (1)-(4) below the main graph were recorded at the corresponding transition points and are normalized relative to the first spectrum (1).

this feature, we switched off the thermoelectric module during the heat-triggered recovery process. As soon as the sample temperature decreased below T_{switch} , the SMP grating froze in its momentary shape. The polymer stayed in this state until its temperature was increased again above T_{switch} and the recovery process continued. Figure 5 reveals this temperature dependence of the recovery process by plotting the change of the peak emission wavelength during this process. The arrows mark the points where heating was switched on and off. The experimental data proves that the laser wavelength stayed constant during the cooling period. After the restart of the heating the peak wavelength changed with approximately the same velocity as before. The accurate response of the polymer to the thermal triggering in this experiment confirms again our previous measurement (Fig. 3b) showing that the UV laser excitation does not influence the shape-memory ability of Tecoflex[®].

4. Conclusion

In conclusion, we demonstrated with an exemplary active optical device that the special abilities of shape-memory polymers work also for nano-sized structures. Utilizing hot embossing we transferred one-dimensional sub-micron gratings into the surfaces of SMP foils and pre-stretched them. In this way, we fabricated a resonator grating with a continuously tunable and adjustable period. The organic semiconductor laser active material Alq₃:DCM together with a pump laser completes the tunable DFB laser device. The threshold and the slope efficiency

of our laser device are comparable to those built on other polymer substrates [35, 36]. The experimental results demonstrate the advantage of SMPs as resonator substrate material for continuously tunable organic distributed feedback lasers. In addition, our DFB laser is not only tunable over a range as wide as 30 nm, it is also flexible. Finally, it does not rely on any mechanical elements or constant power supply as the grating period stays constant after tuning the DFB laser to the chosen emission wavelength.

Due to the shape-memory effect and the optical transparency of the utilized shape-memory polymer Tecoflex[®], such nanostructured SMP foil surfaces offer opportunities to develop tunable optical elements without sophisticated mechanical elements. This will be of interest for many applications where a forward and backward tuning of the wavelength is not essential but reduced volume and costs like medical products for one-time usage. Consequently, SMPs might be used to build individual integrated on-chip organic lasers or complete Lab-on-a-Chip platforms to develop spectrometers for biomedical and chemical point-of-care analysis. Furthermore, coupling of organic lasers to a glass fiber might be actively controlled by using SMP gratings with tunable periods.

Acknowledgments

We thank Tobias Meier, Norbert Schneider, Radwanul H. Siddique, Richard Thelen and all members of the Biomimetics group for their support and helpful discussions. X. L. acknowledges financial support by the Carl Zeiss Stiftung. This work was partly carried out with the support of the Karlsruhe Nano Micro Facility (KNMF, www.kit.edu/knmf), a Helmholtz Research Infrastructure at Karlsruhe Institute of Technology (KIT, www.kit.edu).